Bloch mode analysis of transmission through periodic slit arrays in finite thickness metallic slabs - art. no. 66411S

Article *in* Proceedings of SPIE - The International Society for Optical Engineering · October 2007

DOI: 10.1117/12.733447

CITATION
1

READS
59

4 authors, including:

Aramais Zakharian
Corning Incorporated
134 PUBLICATIONS **2,369** CITATIONS

SEE PROFILE

Masud Mansuripur
The University of Arizona
469 PUBLICATIONS **7,826** CITATIONS

SEE PROFILE

Bloch mode analysis of transmission through periodic slit arrays in finite thickness metallic slabs

Yong Xie, Armis R. Zakharian, Jerome V. Moloney, and Masud Mansuripur

College of Optical Sciences, The University of Arizona, Tucson, Arizona 85721

masud@optics.arizona.edu

Abstract. The Bloch modes of a periodic slit array in a metallic slab are identified, then used to investigate the transmission of light through sub-wavelength slits residing in a finite-thickness slab. Specifically, the Bloch mode method is used here to study Fabry-Perot-like resonances within individual slits, in conjunction with the onset of surface plasmon polariton (SPP) resonances and in the vicinity of the Wood anomalies. Although the results largely agree with our earlier numerical simulations obtained with the Finite-Difference-Time-Domain (FDTD) method, there are indications that the FDTD method has difficulty with convergence at and around resonances; the points of agreement and disagreement between the two methods are discussed in the present paper. When the period p of the slit array is comparable to (or somewhat below) the incident wavelength λ_o, the Bloch mode method requires only the 10-20 lowest-order modes of the slit array to achieve stable solutions; we find the Bloch mode method to be an effective tool for studying dielectric-filled apertures in highly conductive hosts.

Keywords: surface plasmons; polaritons; optics of metals; guided waves; apertures; diffraction theory.

1. Introduction. This paper is a follow-up to our previously published papers [1-4]. The earlier publications addressed the problem of transmission through slits and slit arrays using Finite Difference Time Domain (FDTD) computer simulations as well as an analytic approach based on the expansion of fields into Bloch modes. The goal of the present paper is to extend the Bloch mode method to cover the case of finite-thickness metallic hosts. We also demonstrate that the Bloch mode method can reproduce, rapidly and efficiently, the main features of the FDTD simulations reported in [2] without suffering from the latter's numerical dispersion problems that are most pronounced at and around the various resonances.

The history of grating problems and their resolution dates back to R. W. Wood's famous 1902 paper on the Wood anomalies [5]. Numerous tools have been developed to solve these and related problems; however, there is no single tool that can be generally applied to all cases of interest. Our Bloch mode technique [3, 4] appears to be effective for periodic slit arrays in metallic hosts. Chandezon invented the C-method in 1980 [5], where a new coordinate system for mapping the grating surface onto a plane was introduced; this method works well for surface relief gratings. The coordinate transformation requires derivative continuity along the interface, which is not applicable to our slit arrays at their sharp corners. Moharam and Gaylord developed the Rigorous Coupled Wave Analysis (RCWA) method [7], whose convergence under TM illumination was subsequently improved by Lalanne and Morris [8]. RCWA expands the permittivity function of the periodic structure, $\varepsilon(\omega)$, in a Fourier series. The corresponding eigen-functions, however, do not represent the structure's natural modes, as they are only indirectly related to the sharp material discontinuities at the slit walls. Although the RCWA method is readily applicable to problems associated with the periodic slit arrays, in our studies we have avoided this technique primarily because of our interest in the behavior of the natural modes of the structure.

In a homogeneous environment the eigenfunctions of the wave equation, occasionally referred to as the Rayleigh waves, are a set of plane-waves including both propagating and evanescent

Plasmonics: Metallic Nanostructures and Their Optical Properties V, edited by Mark I. Stockman,
Proc. of SPIE Vol. 6641, 66411S, (2007) · 0277-786X/07/$18 · doi: 10.1117/12.733447

waves. The Rayleigh waves [9] were introduced in 1907 to address the anomalous diffraction from metallic gratings that had been reported by Wood a few years earlier. More recently, the eigen-functions of the slit have been identified and used to analyze the behavior of periodic slit-arrays at optical wavelengths [10]. The difficulty with the modal approach is its rather poor convergence [10], when one attempts to match the boundary conditions using the Rayleigh waves outside, and the slits' Bloch modes inside a high-conductivity material. In our earlier papers we developed an algorithm to obtain the modal coefficients through minimization of the field discontinuities at the interfaces [3, 4]. With this method, we have now successfully obtained the modal amplitudes of all the excited waves (including surface waves) at the metal-dielectric interfaces associated with periodic slit arrays.

Our investigations of sub-wavelength slits in metallic hosts have relied on two methods of computation: (i) FDTD simulations, and (ii) Bloch mode expansion of the fields. The FDTD method employing the perfectly matched boundary layer has been discussed thoroughly and used extensively in the past [11, 12]. We find it instructive to use the Bloch mode approach as a check on the validity of the FDTD results.

This paper begins by describing the equations used in calculating the modal amplitudes. We proceed to calculate the transmittance of the array for different periods and thicknesses. A comparison of our Bloch mode analysis results with the earlier FDTD simulations [2] in section 3 reveals that the two methods are in agreement under fairly general circumstances. Where the two methods disagree, however, we notice that FDTD suffers from convergence problems associated with numerical dispersion.

2. The Bloch mode method. Figure 1 shows a TM-polarized plane-wave at oblique incidence (black arrows) illuminating the top facet of a slit array in a metallic host. The incident beam initially excites two sets of modes: the reflected modes (red arrows), which are the conventional Rayleigh waves, i.e., propagating as well as evanescent plane-waves specified in terms of their field components ($H^n_{xR}, E^n_{yR}, E^n_{zR}$), and downward-propagating Bloch modes within the slab (H^n_{xD}, E^n_{yD}, E^n_{zD}), indicated in the figure with blue arrows. When the downward-propagating Bloch modes reach the bottom facet, they create two additional sets of modes: the transmitted modes (H^n_{xT}, E^n_{yT}, E^n_{zT}), brown arrows, and upward-propagating Bloch modes of the slit array ($H^n_{xU}, E^n_{yU}, E^n_{zU}$), green arrows. Within the slits, the upward and downward modes eventually stabilize after many back-and-forth reflections, creating a Fabry-Perot type of resonant cavity within the individual slits. As may be expected from symmetry, for a given mode-index, the upward and downward modes of the slab should have identical *E*- and *H*-field profiles (aside from a −1 factor multiplying, say, the *E*-field, relating to the fact that the same-index modes propagate in opposite directions.) The Bloch modes of the array may be found by matching the boundary conditions on the (vertical) slit walls, then solving the resulting characteristic equation for the propagation constant. Subsequently, the (complex) mode amplitudes may be obtained by minimizing the discontinuity of the tangential field components at the top and bottom facets of the slit array. Details of this technique, referred to as the Bloch mode method of solving Maxwell's equations for the slit array, have been described in our previous papers [3, 4].

2.1. Slit array equations for a finite thickness metallic slab. In general, an infinite number of modes are needed, both inside and outside the slit array, to account for the material discontinuities and to resolve the strongly localized fields at the sharp slit boundaries. In particular, the tangential E- and H-fields must match at the top and bottom interfaces, as follows:

$$H_{xI} + \sum_{n=1}^{\infty} C_R^n H_{xR}^n = \sum_{n=1}^{\infty} C_D^n H_{xD}^n + \sum_{n=1}^{\infty} \alpha_n C_U^n H_{xU}^n \qquad (1a)$$

$$E_{yI} + \sum_{n=1}^{\infty} C_R^n E_{yR}^n = \sum_{n=1}^{\infty} C_D^n E_{yD}^n + \sum_{n=1}^{\infty} \alpha_n C_U^n E_{yU}^n \qquad (1b)$$

$$\sum_{n=1}^{\infty} C_T^n H_{xT}^n = \sum_{n=1}^{\infty} C_U^n H_{xU}^n + \sum_{n=1}^{\infty} \alpha_n C_D^n H_{xD}^n \qquad (1c)$$

$$\sum_{n=1}^{\infty} C_T^n E_{yT}^n = \sum_{n=1}^{\infty} C_U^n E_{yU}^n + \sum_{n=1}^{\infty} \alpha_n C_D^n E_{yD}^n \qquad (1d)$$

Here C_R^n and C_T^n are the mode amplitudes of the reflected and transmitted Rayleigh waves above and below the slab, while C_U^n and C_D^n are the amplitudes of the upward- and downward-propagating Bloch modes within the slab. α_n is the loss coefficient (including the phase factor) associated with traveling through the thickness τ of the slab. For practical reasons, of course, one must truncate the above series and include only a finite number N of each type of mode.

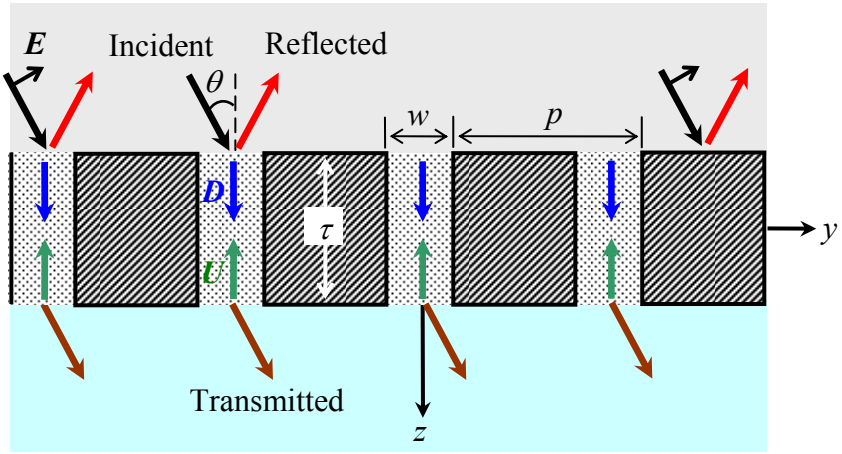

Fig. 1. A TM-polarized plane-wave (H_x, E_y, E_z) arriving at an oblique angle θ illuminates an array of slits in a metallic slab of thickness τ. The incident wavelength is λ_o, the slit width is w, and the array periodicity is p. The incidence medium (gray region above the slab), the transmission medium (light blue, below the slab), the metallic host (slanted shading), and the dielectric filling of the slits (dotted gray) are all homogeneous and isotropic, each having its own dielectric constant ε. The incident beam initiates four sets of modes (Rayleigh waves and Bloch modes) in three regions of space: In the incidence medium, it creates the reflected modes (red arrows); inside the slab (containing the metallic host as well as the dielectric-filled slits), the excitation gives rise to downward- as well as upward-propagating modes (blue and green arrows); the transmitted modes (brown arrows) reside in the light blue region below the slab.

Because the modes of a metallic slit array are not mutually orthogonal, we compute the modal amplitudes C^n through simultaneous minimization of the tangential E- and H-field discontinuities at the top and bottom interfaces [3]. In the error functions f_1 through f_4 listed below, the magnetic field components are weighted by the free-space impedance, $Z_o \approx 377\Omega$, because the H-fields are typically weaker than the corresponding E-field components.

$$f_1 = Z_0^2 [H_{xI} + \sum_{n=1}^{N} (C_R^n H_{xR}^n - C_D^n H_{xD}^n - \alpha_n C_U^n H_{xU}^n)][H_{xI} + \sum_{n=1}^{N} (C_R^n H_{xR}^n - C_D^n H_{xD}^n - \alpha_n C_U^n H_{xU}^n)]^* \qquad (2a)$$

$$f_2 = [E_{yI} + \sum_{n=1}^{N}(C_R^n E_{yR}^n - C_D^n E_{yD}^n - \alpha_n C_U^n E_{yU}^n)][E_{yI} + \sum_{n=1}^{N}(C_R^n E_{yR}^n - C_D^n E_{yD}^n - \alpha_n C_U^n E_{yU}^n)]^* \quad (2b)$$

$$f_3 = Z_0^2 \sum_{n=1}^{N}(-\alpha_n C_D^n H_{xD}^n - C_U^n H_{xU}^n + C_T^n H_{xT}^n)\sum_{n=1}^{N}(-\alpha_n C_D^n H_{xD}^n - C_U^n H_{xU}^n + C_T^n H_{xT}^n)^* \quad (2c)$$

$$f_4 = \sum_{n=1}^{N}(-\alpha_n C_D^n E_{yD}^n - C_U^n E_{yU}^n + C_T^n E_{yT}^n)\sum_{n=1}^{N}(-\alpha_n C_D^n E_{yD}^n - C_U^n E_{yU}^n + C_T^n E_{yT}^n)^* \quad (2d)$$

The total discontinuity may be expressed as $f = f_1 + f_2 + f_3 + f_4$, and an error function may be defined as $Error = \int f \, dy$, where integration is over one full period p of the slit array. The partial derivatives of the error function with respect to the real and imaginary parts of each C_j (i.e., individual mode amplitudes) must be set to zero. This can be shown to be equivalent to treating C_j and its conjugate, C_j^*, as two separate, independent variables, then setting the partial derivatives of the error function with respect to C_j^* equal to zero, that is,

$$\frac{\partial Error}{\partial C_j^*} = \int_{-p/2}^{p/2} \frac{\partial f_1}{\partial C_j^*} + \frac{\partial f_2}{\partial C_j^*} + \frac{\partial f_3}{\partial C_j^*} + \frac{\partial f_4}{\partial C_j^*} dy = 0 \quad (3)$$

Here $\{C_j\} = \{C_R^1, \cdots, C_R^n, C_D^1, \cdots, C_D^n, C_U^1, \cdots, C_U^n, C_T^1, \cdots, C_T^n\}$ represents the set of all modal amplitudes. We obtain the following $4N$ linear equations in $4N$ unknowns (the unknowns being the complex modal amplitudes C_j):

$$\frac{\partial Error}{\partial C_R^{j*}} = \int_{-p/2}^{p/2}\{(Z_0^2 H_{xR}^{j*} H_{xI} + E_{yR}^{j*} E_{yI}) + \sum_{n=1}^{N}[(Z_0^2 H_{xR}^{j*} H_{xR}^n + E_{yR}^{j*} E_{yR}^n) C_R^n - (Z_0^2 H_{xR}^{j*} H_{xD}^n + E_{yR}^{j*} E_{yD}^n) C_D^n$$
$$- (Z_0^2 H_{xR}^{j*} \alpha_n H_{xU}^n + E_{yR}^{j*} \alpha_n E_{yU}^n) C_U^n]\} dy \quad (4a)$$

$$\frac{\partial Error}{\partial C_D^{j*}} = \int_{-p/2}^{p/2}\{-(Z_0^2 H_{xD}^{j*} H_{xI} + E_{yR}^{j*} E_{yI}) + \sum_{n=1}^{N}\{-(Z_0^2 H_{xD}^{j*} H_{xR}^n + E_{yD}^{j*} E_{yR}^n) C_R^n + [(Z_0^2 H_{xD}^{j*} H_{xD}^n + E_{yD}^{j*} E_{yD}^n)$$
$$+ (Z_0^2 \alpha_j^* H_{xD}^{j*} \alpha_n H_{xD}^n + \alpha_j^* E_{yD}^{j*} \alpha_n E_{yD}^n)] C_D^n + [(Z_0^2 H_{xD}^{j*} \alpha_n H_{xU}^n + E_{yD}^{j*} E_{yU}^n) + (Z_0^2 \alpha_j^* H_{xD}^{j*} H_{xU}^n$$
$$+ \alpha_j^* E_{yD}^{j*} E_{yU}^n)] C_U^n - (Z_0^2 \alpha_j^* H_{xD}^{j*} H_{xT}^n + \alpha_j^* E_{yD}^{j*} E_{yT}^n) C_T^n\}\} dy \quad (4b)$$

$$\frac{\partial Error}{\partial C_U^{j*}} = \int_{-p/2}^{p/2}\{-(Z_0^2 \alpha_j^* H_{xU}^{j*} H_{xI} + \alpha_j^* E_{yU}^{j*} E_{yI}) + \sum_{n=1}^{N}\{-(Z_0^2 \alpha_j^* H_{xU}^{j*} H_{xR}^n + \alpha_j^* E_{yU}^{j*} E_{yR}^n) C_R^n + [(Z_0^2 \alpha_j^* H_{xU}^{j*} H_{xD}^n$$
$$+ \alpha_j^* E_{yU}^{j*} E_{yD}^n) + (Z_0^2 H_{xU}^{j*} \alpha_n H_{xD}^n + E_{yU}^{j*} \alpha_n E_{yD}^n)] C_D^n + [(Z_0^2 \alpha_j^* H_{xU}^{j*} \alpha_n H_{xU}^n + \alpha_j^* E_{yU}^{j*} \alpha_n E_{yU}^n)$$
$$+ (Z_0^2 H_{xU}^{j*} H_{xU}^n + E_{yU}^{j*} E_{yU}^n)] C_U^n - (Z_0^2 H_{xU}^{j*} H_{xT}^n + H_{xU}^{j*} H_{xT}^n) C_T^n\}\} dy \quad (4c)$$

$$\frac{\partial Error}{\partial C_T^{j*}} = \int_{-p/2}^{p/2}\{\sum_{n=1}^{N}[-(Z_0^2 H_{xT}^{j*} \alpha_n H_{xD}^n + E_{yT}^{j*} \alpha_n E_{yD}^n) C_D^n - (Z_0^2 H_{xT}^{j*} H_{xU}^n + E_{yT}^{j*} E_{yU}^n) C_U^n + (Z_0^2 H_{xT}^{j*} H_{xT}^n + E_{yT}^{j*} E_{yT}^n) C_T^n]\} dy \quad (4d)$$

The above set of linear equations in the $4N$ unknown mode amplitudes $\{C_j\}$ can be readily solved by inverting the $4N \times 4N$ coefficients matrix.

2.2 Simplified equations in the case of a thick slab. When the slit-width w is below one half of one wavelength, one and only one TM-polarized Bloch mode propagates through the depth of the slit; all the other modes decay rapidly and, assuming the slab thickness τ is greater than the skin-depth

of the metallic medium, none of these other modes retains a significant amplitude at the opposite facet of the slab. Thus, if the slab is thick enough to be opaque, one can generally ignore the contribution of all but one of the Bloch modes (i.e., the long-range guided mode) at the facet of the slab opposite the point of origination of the mode. Under such circumstances, one does not need to solve the entire set of $4N$ linear equations (4); rather, the three sets of linear equations listed below as Eqs. (5), each having $2N$ unknowns, should suffice. The first two of these equations, (5a, 5b), represent incidence from the top on a semi-infinite slab; see Ref. [3]; Eqs. (5c, 5d) correspond to the case of a downward-propagating guided mode arriving at the bottom facet; Eqs. (5e, 5f) represent the case of an upward-propagating guided mode arriving (from below) at the top interface.

$$H_{xI} + \sum_{n=1}^{\infty} C_R^n H_{xR}^n = \sum_{n=1}^{\infty} C_D^n H_{xD}^n \qquad (5a)$$

$$E_{yI} + \sum_{n=1}^{\infty} C_R^n E_{yR}^n = \sum_{n=1}^{\infty} C_D^n E_{yD}^n \qquad (5b)$$

$$H_{xD}^1 + \sum_{n=1}^{\infty} C_U^n H_{xU}^n = \sum_{n=1}^{\infty} C_T^n H_{xT}^n \qquad (5c)$$

$$E_{yD}^1 + \sum_{n=1}^{\infty} C_U^n E_{yU}^n = \sum_{n=1}^{\infty} C_T^n E_{yT}^n \qquad (5d)$$

$$H_{xU}^1 + \sum_{n=1}^{\infty} C'^n_D H_{xD}^n = \sum_{n=1}^{\infty} C'^n_R H_{xR}^n \qquad (5e)$$

$$E_{yU}^1 + \sum_{n=1}^{\infty} C'^n_D E_{yD}^n = \sum_{n=1}^{\infty} C'^n_R E_{yR}^n \qquad (5f)$$

In the steady-state, we assume that the first Bloch mode of the slit array, which is the only guided mode that propagates downward, has amplitude a at the top interface. Similarly, the upward propagating guided mode has amplitude b at the bottom interface. We also define ρ as the attenuation factor (including phase) of the guided mode when it travels through the thickness τ of the slab. According to Eqs. (5c, 5d), the amplitude b is obtained by reflection of the downward-propagating guided mode at the bottom facet; therefore, $b = a\rho C_U^1$. The amplitude a consists of two parts: one part, according to Eqs. (5a, 5b), is created by the incident beam, that is, C_D^1; the other, resulting from the reflection of the upward-propagating guided mode at the top facet is given, in accordance with Eqs. (5e, 5f), by $b\rho C'^1_D$. Consequently,

$$a = C_D^1 + a\rho C_U^1 \rho C'^1_D \qquad (6)$$

The amplitudes of the two guided modes at the top and bottom facets will thus be

$$a = \frac{C_D^1}{1 - \rho^2 C_U^1 C'^1_D} \qquad (7a)$$

$$b = a\rho C_U^1 = \frac{\rho C_D^1 C_U^1}{1 - \rho^2 C_U^1 C'^1_D} \qquad (7b)$$

Having determined the guided mode amplitudes at the top and bottom interfaces, one can now compute the other mode amplitudes using Eqs. (5a-5f).

3. Comparison of FDTD simulations with results obtained by the Bloch mode method. In a previous paper [2] we used FDTD simulations to study the transmission of light through periodic slit arrays as function of the slab thickness τ and array periodicity p. With the results of the Bloch mode method at hand, we are now in a position to compare the two methods. Since FDTD integrates Maxwell's equations in time, it has an intrinsic error due to numerical dispersion. Our intent here is not to investigate such errors in any detail; rather we point out the consequences of this type of error in the vicinity of strong resonances, and show the superiority of the Bloch mode method under resonance conditions. We mention in passing that the newly discovered FDTD errors do *not* change the general conclusions reached in our previous publication, Ref. [2], although they do modify the numerical values of the transmission efficiency η in the vicinity of SPP and Fabry–Perot resonances as well as those near the Wood anomalies.

The setup for the simulations is the same as that used in Ref. [2], namely, a periodic slit array with variable period p, fixed slit-width $w = 0.1\,\mu m$, in a silver slab (thickness $= \tau$, $\varepsilon_m = -48.8 + 3.16i$ at $\lambda_o = 1.0\ \mu m$), illuminated at normal incidence by a TM-polarized plane-wave (i.e., H-field parallel to the slit's long axis). The normalized transmittance η is defined as the ratio of the transmitted optical power (i.e., component S_z of the Poynting vector along z) integrated over a full period p, divided by the incident optical power integrated over the width w of a single slit. To compare the two methods of calculation, we examine three cases in Table 1: (i) $p = 0.5\mu m$, which is far below both the SPP resonance and the Wood anomaly; (ii) $p = 0.99\ \mu m$, at the SPP resonance; (iii) $p = 1.0\mu m$, at the Wood anomaly. The slab thickness is fixed at $\tau = 0.7\mu m$ in all three cases.

Table 1. Normalized transmittance in three cases, calculated with FDTD and with the Bloch mode method

p (μm)	η (Bloch mode)	η (FDTD, using different simulation times T)					
		$T = 100\ fs$	$200\ fs$	$400\ fs$	$1100\ fs$	$2200\ fs$	$5600\ fs$
0.50	**2.99**	**2.984**	**2.982**	**2.982**	**2.984**	**2.983**	**2.983**
0.99	**4.0e-5**	**-0.057**	**-0.011**	**0.011**	**0.005**	**0.004**	**0.000**
1.00	**2.46**	**0.223**	**0.656**	**1.070**	**2.013**	**2.743**	**1.690**

For $p = 0.5\ \mu m$, the results obtained with the two methods differ only by about 0.2%; the FDTD in this case converges in less than 100 *fs*, which is the time needed for about 10 round-trips of the surface waves between adjacent slits. For $p = 0.99\mu m$, the FDTD results for short simulation times are obviously wrong ($\eta < 0$); for long simulations, the results eventually converge, but this takes quite a long time (over 5 *ps*), corresponding to more than 700 round-trips of the surface waves. For $p = 1.0\mu m$, the FDTD results are unstable and continue to oscillate around the value predicted by the Bloch mode method. In other words, in the vicinity of resonances, FDTD has problems with convergence, requiring extremely long simulations for the behavior to settle down.

In Fig. 2 plots of normalized transmittance η obtained with the Bloch mode method (top) and with FDTD simulations (bottom) are shown using the same color scale. We see that the blue, green, and yellow bands, which cover most of the plot area, show similar trends and match quite well in the two sets of calculations. The Wood anomalies, at $p = 1.0\ \mu m$ and $p = 2.0\ \mu m$, are clearly visible in the Bloch mode plot, but are absent from (or blurred in) the FDTD plot; the FDTD simulations at these anomalous points apparently did not run long enough to stabilize. Upon increasing the period p, as the SPP resonances at $p = 0.99\mu m$ and $p = 1.98\mu m$ are approached from below, the high transmissivity bands (yellow and red) obtained with FDTD show discontinuities, a behavior that is

absent from the results of the Bloch mode method. Finally, when the slab thickness τ is at or near its optimum value for a given period p, the maximum values of η predicted by the FDTD simulations (red bands) are somewhat greater than those predicted by the Bloch mode method.

In the year 2004, with forty fast processors working in parallel, the FDTD simulations shown in Fig. 2 (bottom frame) took nearly two months to complete. These simulations were done blindly, because, at that time, we did not know where to pay attention to convergence. With the Bloch mode method, however, the job of computing the top frame of Fig. 2 on a personal computer was completed in only two days. Needless to say, the latter approach allows finer resolution and higher precision as well.

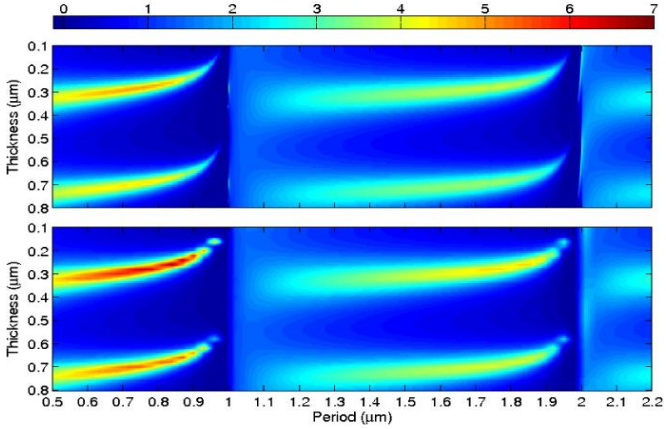

Fig. 2. Color-coded map of normalized transmittance η obtained using the Bloch mode method (top), and FDTD simulations (bottom). In each case the horizontal axis depicts the period p of the slit array, while the vertical axis represents the thickness τ of the silver slab. The slit-width is fixed at $w = 0.1\mu$m, and the TM-polarized, normally incident plane-wave has $\lambda_o = 1.0$ μm. SPP resonances occur at $p = 0.99\mu$m and 1.98μm, while the Wood anomalies are at $p = 1.0$ μm and 2.0 μm.

4. Fabry-Perot cavity formed by internal reflections at the slit's entrance and exit facets. In our FDTD simulations we noticed that, when the period p approaches λ_{spp}, the Fabry-Perot resonances become more apparent, that is, for a fixed value of p, the plot of the transmission efficiency versus slab thickness τ becomes narrower around the peak value $\eta_{\max}$; see Fig. 2. Since FDTD simulations are time-consuming, the details of the behavior near resonances could not be checked in our previous paper [2]. With the Bloch mode technique working efficiently, we can now analyze the dependence of η on τ for different values of the period p. Figure 3 shows plots of the normalized transmittance η versus τ for different values of the period p of the slit array. At $p = 0.8\lambda_o$ the peaks are tall and broad, but in the vicinity of the surface plasmon resonance at $p \sim 0.99\lambda_o$, transmission peaks all but disappear. Immediately beyond the SPP resonance lies the Wood anomaly at $p = \lambda_o$, where the transmission peaks re-appear. Note that the peaks that occur at large thickness ($\tau > 0.5$ μm) are somewhat weaker than those that appear in a thin slab ($\tau < 0.5$ μm), the reason being the increased absorption within the slit walls of the thicker slabs.

5. Concluding remarks. The Bloch mode method is a robust and efficient technique for computing the optical properties of periodic slit arrays in metallic hosts. The Bloch mode profiles and their associated propagation constants are obtained by solving the Maxwell equations within the slits and in the metallic regions between adjacent slits [3, 4]. The modal amplitudes (i.e., complex coupling coefficients) are then determined by minimizing the *E*- and *H*-field discontinuities at the entrance and exit facets of the array (i.e., at the interfaces with the incidence and transmittance environments). The Bloch mode method solves the problem efficiently, without suffering from the numerical dispersion problem associated with FDTD simulations. In contrast, the FDTD method can be used extensively in photonic simulations involving non-periodic and/or complex geometries, provided that special attention is paid to convergence under resonance conditions.

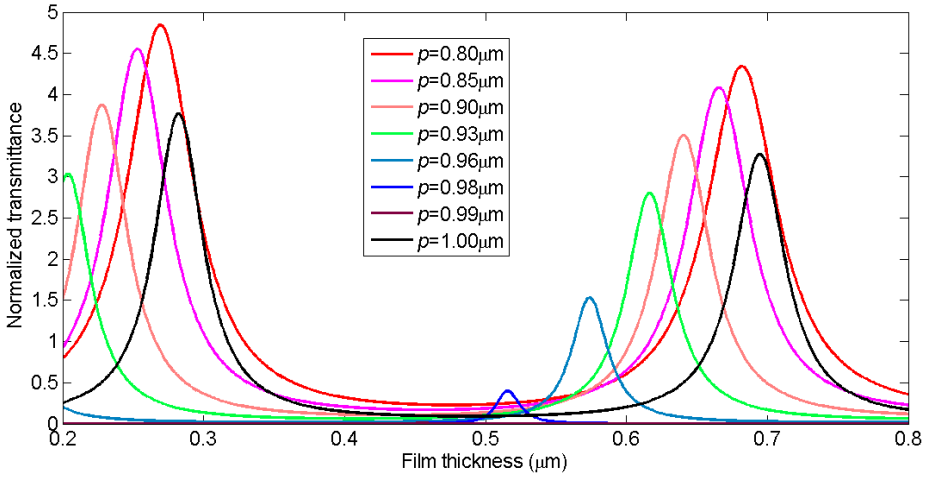

Fig. 3. Normalized transmittance η versus the slab thickness τ for different values of the period p of the slit array. At $p = 0.8\lambda_o$ the peaks are tall and broad, but in the vicinity of the surface plasmon resonance at $p \sim 0.99\lambda_o$, transmission peaks all but disappear. Immediately beyond the SPP resonance lies the Wood anomaly at $p = \lambda_o$, where the transmission peaks re-appear.

Acknowledgements. The authors are grateful to Moysey Brio, John Weiner, Krishna Gundu, Philippe Lalanne, and Hongbo Li for many helpful discussions. JVM acknowledges support from the Alexander von Humboldt Foundation. This work has been supported by the AFOSR contracts F49620-03-1-0194, FA9550-04-1-0213, FA9550-04-1-0355 awarded by the Joint Technology Office.

References

1. Y. Xie, A. R. Zakharian, J. V. Moloney, and M. Mansuripur, "Transmission of light through slit apertures in metallic films," Opt. Express **12**, 6106-21 (2004).
2. Y. Xie, A. R. Zakharian, J. V. Moloney, and M. Mansuripur, "Transmission of light through a periodic array of slits in a thick metallic film," Opt. Express **13**, 4485-91 (2005).
3. Y. Xie, A. R. Zakharian, J. V. Moloney, and M. Mansuripur, "Transmission of light through periodic arrays of sub-wavelength slits in metallic hosts," Opt. Express **14**, 6400-13 (2006).
4. Y. Xie, A. R. Zakharian, J. V. Moloney, and M. Mansuripur, "Optical transmission at oblique incidence through a periodic array of sub-wavelength slits in a metallic host," Opt. Express **14**, 10220-27 (2006).
5. R. W. Wood, "On a remarkable case of uneven distribution of light in a diffraction grating spectrum," Proc. Phys. Soc. London **18**, 269-275 (1902).
6. J. Chandezon D. Maystre, G.Raoult, "A new theoretical method for diffraction gratings and its numerical application," J. Optics (Paris), **11**(4), 235-241 (1980).
7. M. G. Moharam, T. K. Gaylord, "Rigorous coupled-wave analysis of metallic surface-relief gratings," J. Opt. Soc. Am. A **3**(11), 1780-1787 (1986).
8. Ph. Lalanne and G. M. Morris, "Highly improved convergence of the coupled-wave method for TM polarization," J. Opt. Soc. Am. A **13**, 779-784 (1996).
9. Lord Rayleigh, "On the dynamic theory of gratings", Proc. R. Soc. A **79**, 399-416 (1907).
10. L. Li, "A modal analysis of lamellar diffraction gratings in conical mountings," J. Modern Optics **40**(4), 553-73 (1993).
11. K. S. Yee, "Numerical solution of initial boundary value problems involving Maxwell's equations in isotropic media," IEEE Trans. Antennas and Propagation **14**(3), 302-7 (1966).
12. J. P. Berenger, "Three-dimensional perfectly matched layer for the absorption of electromagnetic waves," Journal of Computational Physics **127**, 363-379 (1996).